

Influence of Material State on Austenitic Transformation in HSLA-Type Steel

Anna Wojtacha^{1*}, Mateusz Morawiec², Marek Opiela¹

¹ Faculty of Mechanical Engineering, Silesian University of Technology, Department of Engineering Materials and Biomaterials, ul. Konarskiego 18A, 44-100 Gliwice, Poland

² Faculty of Mechanical Engineering, Silesian University of Technology, Materials Research Laboratory, ul. Konarskiego 18A, 44-100 Gliwice, Poland

* Corresponding author's e-mail: anna.wojtacha@polsl.pl

ABSTRACT

The paper presents the results of research on the influence of the material condition – HSLA steel with Ti and Nb microadditions – on the course of the austenitic transformation. In order to determine the kinetics of phase transformations occur in steel during individual stages of the austenitic transformation, tests were carried out using a Bähr 805 A/D dilatometer. In turn, the influence of hot plastic deformation on the course of the austenitic transformation, were determined via plastometric tests carried out using the Gleeble 3800 thermomechanical simulator. For detailed microstructural analysis, microscopic examinations were carried out using the light microscope and the scanning electron microscope. The obtained results were compared with hardness measurements. The tests carried out showed significant differences in the course of the austenitic transformation and the values of critical temperatures for steel before and after using the plastic deformation. The A_{c1} temperature for steel in the as-cast state is 850 °C and the A_{c3} temperature is 950 °C. As the annealing temperature increases, the hardness increases from 210 HV100 for a temperature of 700 °C to 260 HV100 for a temperature of 920 °C. Knowledge about the phase transformations of supercooled austenite is extremely important, especially for newly developed steels, hence the aim of the work was to analyze the atypical course of the austenitic transformation of HSLA steels and to determine the influence of deformation on the austenitic transformation during heating.

Keywords: HSLA-type steel, austenitic transformation, dilatometry, thermomechanical simulation.

INTRODUCTION

The manufacturing of high-quality steel products dedicated to the automotive, machinery and mining industries is a challenge for manufacturers due to various technological difficulties. The topics of scientific and research works and the directions of development of forging technologies focus on the possibility of producing forgings with the lowest possible weight and with the lowest possible production costs [1, 2]. The combination of appropriately selected thermomechanical conditions and a rationally selected chemical composition allows obtaining a fine-grained structure, which determines high strength

and plastic properties and guaranteed resistance to brittle fracture [3–5].

HSLA-type structural steels are particularly useful for manufacturing products with a fine-grained structure using thermomechanical processing methods, i.e. under regulated conditions of hot plastic deformation and controlled cooling, directly from the hot plastic deformation temperature with subsequent high tempering [6, 7]. Such technological solutions ensure high quality of products and a significant reduction in production costs due to the elimination of energy-intensive heat treatment operations or its limitation only to tempering [8]. The most serious problems related to the weldability of this steel are cracking in the

weld and the heat-affected zone, in particular the problem of hydrogen-induced cracking, due to its high hardenability. Cold cracking is caused by residual stresses and hydrogen diffusion during the welding process, at low temperatures (below 150 °C). The process of welding thick sheets of HSLA steel poses a high risk of cold cracking [9, 10].

Correct design of thermomechanical treatment technology requires knowledge of the transformation diagrams of supercooled austenite and the critical temperatures of steel, i.e. A_{c3} , A_{cl} and M_s . Commercial software is of great technical usefulness, enabling, among others, to determine phase evolution diagrams in equilibrium conditions and simulate austenite phase transformations in non-equilibrium conditions and determine CCT (continuous cooling transformations) and TTT (temperature time transformation) diagrams [11–13]. Issues related to the influence of plastic deformation on the material in its initial state and the kinetics of phase transformations in HSLA-type steels were the subject of research in works [14–17]. Especially for newly developed steels, the knowledge about the phase transformations of supercooled austenite is extremely important. Very few reports in the literature concern the analysis of the kinetics of phase transformations of supercooled austenite in this group of steels in the as-cast state. Therefore, the aim of this work was to analyze the unusual course of austenitic transformation for HSLA-type steel in the as-cast state, and in particular to try to explain the obtained

values of critical temperatures, which differ significantly from typical values for alloys with a similar chemical composition. Additionally, the study determined the influence of deformation on the austenitic transformation during heating.

MATERIALS AND METHODS

The chemical composition of the newly developed HSLA steel is shown in Table 1. Ingots with a diameter of 30 mm and a length of 400 mm were made in an electric induction furnace VEM I20. The chemical composition of the ingots was determined using a LECO GDS500A glow discharge emission spectrometer.

Dilatometric tests were carried out using a BÄHR 805 A/D dilatometer with induction heating and a vacuum chamber. Samples with a diameter of 4 mm and a length of 10 mm were heated at a rate of 3 °C/s to individual temperatures ranging from 700 °C to 1000 °C. Next, samples were held at the given temperatures for 300 s, and then cooled at a rate of 60 °C/s to ambient temperature. The cooling medium used was helium. The determination of the start and end temperatures of phase transformations was carried out in accordance with the ASTM A1033-04 standard [18]. The diagram of the conducted experiment is shown in Figure 1a. In order to determine the influence of hot plastic deformation on the course of the austenitic transformation and the A_{cl} and

Table 1. Chemical composition of the analyzed steel [wt.%]

C	Mn	Si	P	S	Cr	Mo	Ti	Nb
0.178	1.94	1.12	0.014	0.019	0.028	0.198	0.011	0.035

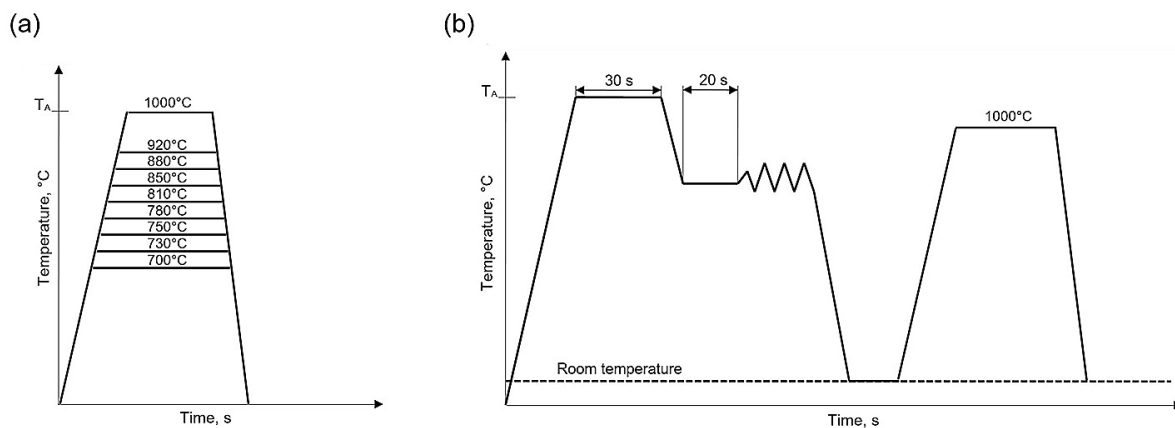


Figure 1. Scheme of carrying out dilatometric (a) and plastometric tests (b)

A_{c3} temperature values, plastometric tests were carried out using a Gleeble 3800 thermomechanical simulator. The tested axisymmetric cylindrical sample with a diameter of 10 mm and a length of 15 mm was resistively heated in a vacuum at a rate of 3 °C/s to the austenitizing temperature 1150 °C, held for 30 s and cooled to a plastic deformation temperature of 1100 °C. Continuous compression of the sample was carried out at a strain rate of 10s⁻¹ to a strain of 0.7. After initial hot forming, the sample was heated again in a dilatometer to a temperature of 1000 °C, annealed for 300 s and cooled to room temperature (Fig. 1b). In order to eliminate the effects caused by changes in test parameters, identical cooling conditions were used as in the case of as-cast samples (cooling at a rate of 60 °C/s to ambient temperature). All parameters used in the tests were selected on the basis of typical parameter ranges used in thermomechanical treatment for forgings produce of HSLA-type steel.

Then, samples were prepared for metallographic tests. The samples were cut to one third of their length and embedded in resin. In order to reveal the structure, after conventional preparation (grinding and polishing), the samples were etched with 5% nital. Metallographic examinations were performed using an Observer.Z1m optical microscope from Zeiss at 200x magnification and a SUPRA 25 scanning electron microscope from Zeiss. The samples after dilatometric tests were tested for hardness using the Vickers method (Future-Tech FM-700 hardness tester) at a load of 1000 kgf. Hardness measurements were carried out in accordance with the applicable PN-EN ISO 6507-1 standard. Hardness

measurements were carried out with a load of 1000kgf in order to determine the hardness on the largest possible sample surface (hardness of material not the phase). Hardness was measured on metallographic specimens; five measurements were made for each variant. Standard deviation values were added for the obtained results.

RESULTS

The obtained dilatometric curves are shown in Figure 2. The obtained results indicate significant differences in the course of the austenitic transformation. In the case of as-cast steel at a temperature of 730 °C, a change in the curve can be observed, followed by an increase in sample elongation, which cannot be equated with the beginning of the austenitic transformation (the formation of austenite is accompanied by a decrease in volume). The sample elongation decreases only after exceeding the temperature of 850 °C, indicating the beginning of the austenitic transformation, which ends at a temperature of approximately 950 °C. The course of the austenitic transformation for a sample compressed at a strain rate of 10s⁻¹ indicates that the critical temperatures are $A_{c1} = 750$ °C and $A_{c3} = 940$ °C. This course of austenitic transformation and the values of critical temperatures are characteristic for this type of steel with a similar chemical composition [19–22].

In the case of steel in the as-cast state, at a temperature of approximately 730 °C, there was an increase in the length of the sample, which was probably caused by the dissolution of cementite.

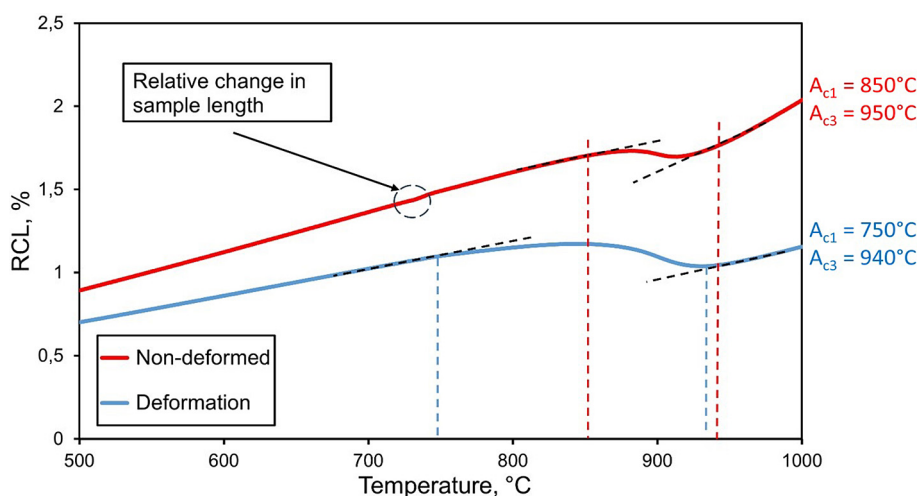


Figure 2. Dilatometric curves of the austenitic transformation during heating of the tested steel in the as-cast state and after applying plastic deformation

No changes were observed in the obtained curve until the temperature of 850 °C was reached, indicating the beginning of the austenitic transformation, which ends at approximately 950 °C.

Carrying out the intercritical annealing process of steel in the as-cast state at various temperatures allowed determining whether the shares between ferrite and austenite change from 730 °C or only when the temperature reaches 850 °C. Microscopic comparison between the initial microstructure (Fig. 3) and the microstructure at various temperatures (Fig. 4) fully correlate with the results of dilatometric tests. The higher the intercritical annealing temperature, the more the share of coarse-grained ferrite begins to decrease and the share of martensite formed from austenite begins to increase. These results confirm the slower course of the austenitic transformation and the need to use higher temperatures.

Figure 5 shows microstructures obtained using a scanning electron microscope. At a temperature of 700 °C, the structure shows mainly ferrite with some martensite and cementite in the form of spherical precipitates in block grains. The presence of cementite means that the A_{c1} temperature was not exceeded. Increasing temperature to 730 °C causes the cementite to dissolve (which correlates with the increase in elongation on the dilatometric curve) while maintaining the ferritic-martensitic structure. Further increase in temperature causes complete dissolution of cementite

and reduction of the ferrite grain size with an increase in the share of block martensite. From a temperature of 810 °C, bainitic ferrite appears in the microstructure, the presence of which is caused by the high concentration of silicon in the steel. Additionally, martensitic-austenitic islands are visible in the structure. Further increasing the temperature leads to further fragmentation of the ferrite, with an increase in the proportion of bainitic ferrite. Martensite blocks and martensitic-austenitic islands are also visible. Increasing the temperature is also accompanied by an increase in the share of retained austenite at the grain boundaries in the form of blocks, and at temperatures higher than 850 °C also in the form of thin laths. The presence of martensite in microstructure is the result of low thermal stability of austenite, present during isothermal holding. Low amount of austenitizing element in the chemical composition of the steel, does not allow for austenite to be fully stable (because of small amount of carbon and manganese). The presence of martensite at temperatures between 700–810 °C, could mean that a non-detectable amount of austenite is formed during the isothermal holding, which during cooling undergo martensite transformation. Moreover, local dissolution of carbides at 700 °C, could enrich the area with carbon, which locally could decrease the A_{c1} temperature, resulting in formation of small amount of austenite. Figure 6 shows that hot plastic deformation resulted



Figure 3. Microstructure of the as-cast steel composed of δ ferrite in the shape of bright with grains, α ferrite formed from the austenite as small grains and small amount of martensite

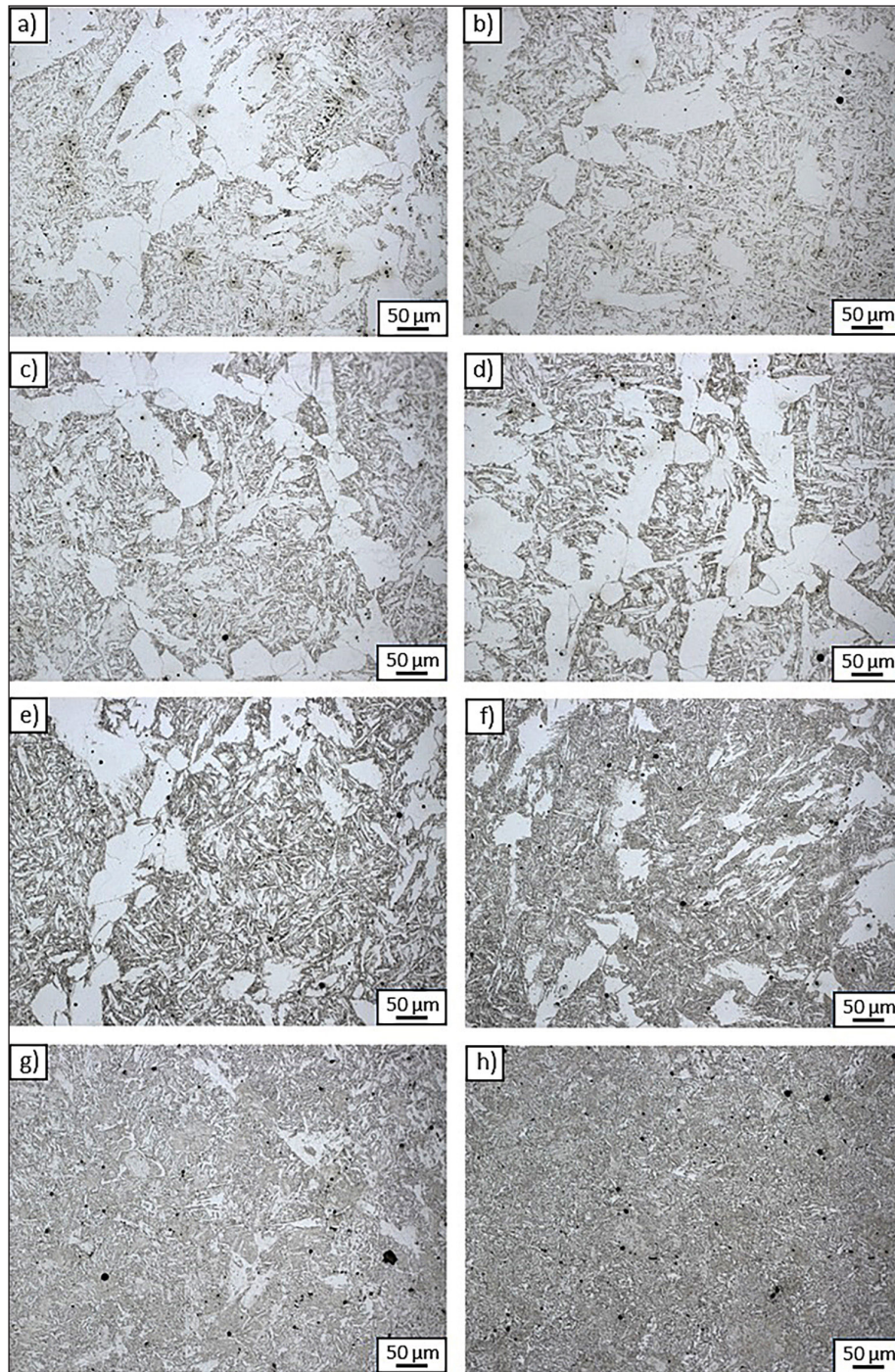


Figure 4. Microstructure of steel in the as-cast state after intercritical annealing at a temperature: (a) 700 °C, (b) 730 °C, (c) 750 °C, (d) 780 °C, (e) 810 °C, (f) 850 °C, (g) 880 °C, (h) 920 °C

in significant fragmentation of the microstructure. The structure is homogeneous and consists mainly of ferrite, bainitic ferrite and martensitic-austenitic islands. The last stage of the research was the measurement of the hardness of steel in the as-cast state using the Vickers method. The hardness measurement results are shown in Figure 7. The hardness of the steel as delivered is 229 HV100. In the heat treatment process with

annealing at 700 °C and 730 °C, hardness was 210 HV100 and 208 HV100, respectively. The slight reduction in hardness may be due to the dissolution of the cementite. With further increases in heating temperatures in the heat treatment process to 750 °C, 780 °C and 810 °C, hardness initially increased by 13 HV100 and then slightly to 224 HV100 for 810 °C. This may indicate the appearance of a small amount of a higher hardness

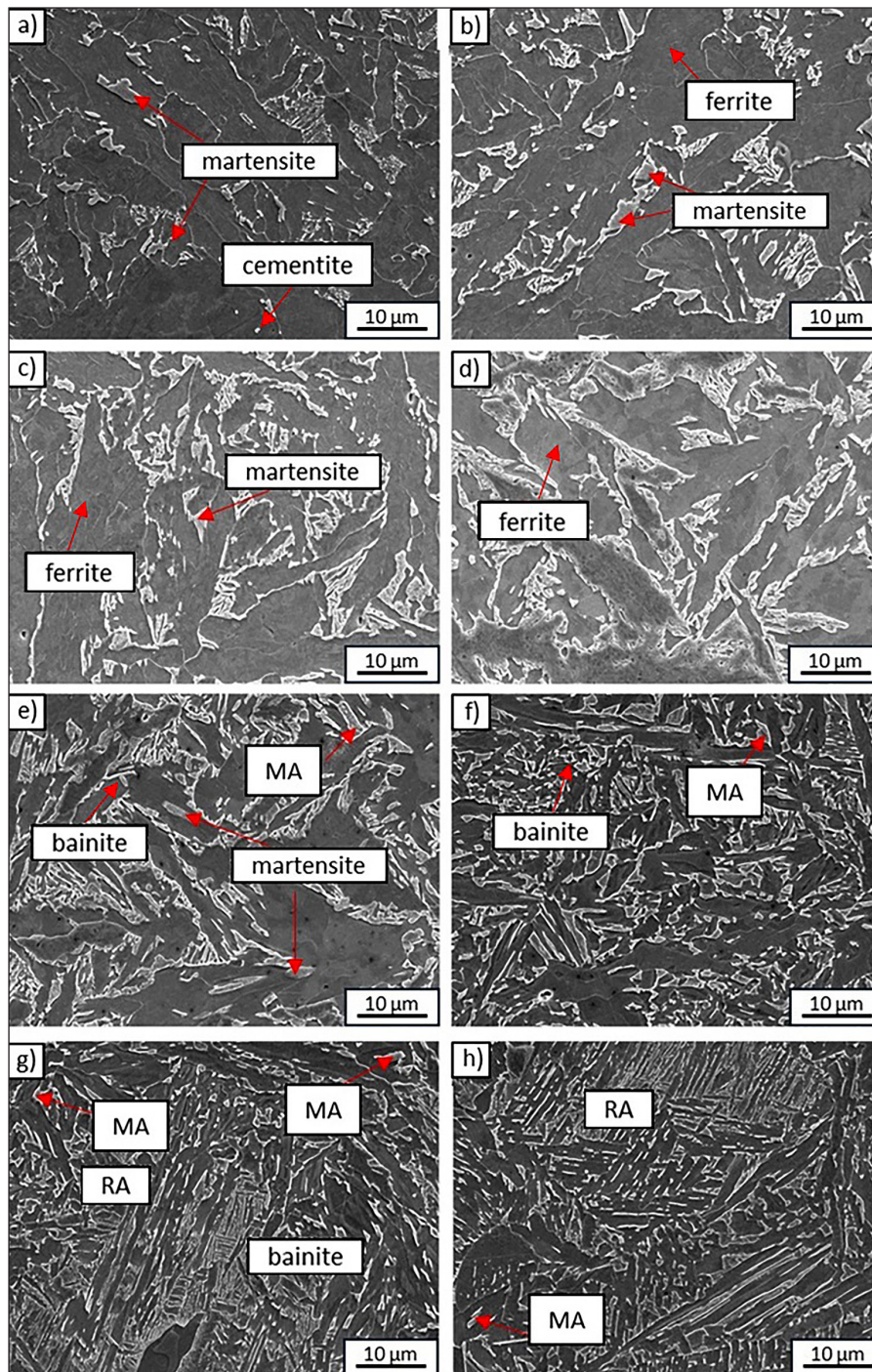


Figure 5. Microstructure of steel in the as-cast state after intercritical annealing at a temperature: a) 700°C, b) 730°C, c) 750°C, d) 780°C, e) 810°C, f) 850°C, g) 880°C, h) 920°C

phase, such as bainite or martensite. With a further increase in the heating temperature to 850 °C, hardness increases slightly (230 HV100), and when this temperature is exceeded, hardness increases significantly. For temperatures of 880 °C and 920 °C, an increase in hardness to 245 HV100 and 260 HV100 was observed. This phenomenon indicates a more intense austenitic transformation in this temperature range. During cooling, a large

amount of austenite is transformed into phases with higher hardness, including bainite, which affects the overall hardness of the steel. The hardness tests carried out confirm that the A_{c1} temperature is approximately 850 °C (in the case of steel in the as-cast state), and the formation of austenite is initially long and slow, and then the rate of transformation into austenite increases after the temperature exceeds 850 °C.

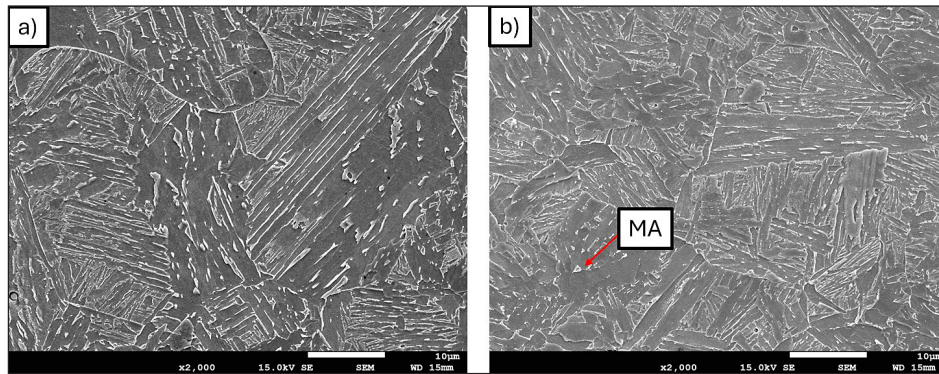


Figure 6. Steel microstructure: (a) in as-cast state, (b) after dilatometric tests and hot plastic deformation (austenitizing temperature = 1150 °C, deformation rate = 10 s⁻¹, deformation value = 0.7)

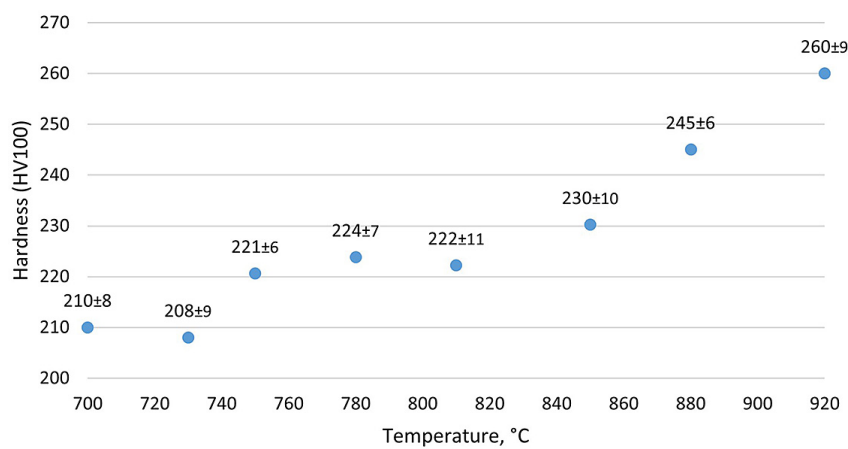


Figure 7. Diagram of changes in the hardness measurement

DISCUSSION

The literature analysis showed that the temperature ranges for the beginning of the austenitic transformation (A_{c1} temperature) and for achieving the full austenite microstructure (A_{c3} temperature) are approximately 700–800 °C and approximately 820–910 °C, respectively, for HSLA-type steels with similar chemical composition [20–29]. Table 2 lists the experimentally determined A_{c1} and A_{c3} temperature values for selected HSLA-type steels with a chemical composition similar to the steel being tested.

Plastic deformation of austenite resulted in an increase in dislocation density and strengthening as a result of grain refinement (Fig. 6). The application of deformation accelerated the onset of the austenitic transformation. Du et al. [30] confirmed that the diffusion transformation in which austenite is separated from hypoeutectoid ferrite occurs faster as a result of deformation. Due to the increase in the density of defects,

such as dislocations and deformation bands in non-recrystallized austenite, the deformation effectively increases the phase transformation rate $\alpha \rightarrow \gamma$ by increasing the preferred nucleation sites of austenite and leads to a decrease in the phase transformation temperature [31].

In the case of steel in the as-cast state, dendrites can be observed in the microstructure, which indicates the occurrence of segregation of the chemical composition. The greater the dendritic segregation, the lower the diffusion coefficient of the components in the melt. The applied plastic deformation at high temperature significantly accelerated the diffusion process, which resulted in the homogenization of the structure [32]. The detailed microstructural analysis carried out indicates the need to apply plastic deformation processing of steel.

Steel in the as-cast state is characterized by greater hardness due to the presence of a heterogeneous structure. Oliveira et al. [33] showed that the HSLA-type steel they tested in the as-cast

Table 2. Experimentally determined A_{c1} and A_{c3} temperature values for selected HSLA-type steels [18–27]

No.	Chemical composition	Temperature values A_{c1} and A_{c3}	Literature item
1.	0.09% C, 1.27% Mn, 0.06% Cr, 0.26% Si, 0.03% Mo, 0.04% V i 0.02% Nb	$A_{c1} = 730\text{ }^{\circ}\text{C}$ $A_{c3} = 910\text{ }^{\circ}\text{C}$	[20]
2.	0.089% C, 0.21% Si, 1.4% Mn, 0.131% Mo, 0.018% Ti, 0.029% Nb i 0.0021% B	$A_{c1} = 702\text{ }^{\circ}\text{C}$ $A_{c3} = 834\text{ }^{\circ}\text{C}$	[21]
3.	0.047% C, 1% Mn, 5.94% Ni, 2.38% Cu, 1.7% Cr, 0.49% Mo, 0.55% Al., 0.167% V, 0.047% Nb	$A_{c1} = 672\text{ }^{\circ}\text{C}$ $A_{c3} = 850\text{ }^{\circ}\text{C}$	[22]
4.	0.09% C, 0.29% Si, 1.40% Mn, 0.011% P, 0.004% S, 0.018% Al, 0.016% Ti, 0.041% V, 0.0074% N	$A_{c1} = 759\text{ }^{\circ}\text{C}$ $A_{c3} = 856\text{ }^{\circ}\text{C}$	[23]
5.	0.08% C, 0.29% Si, 1.40% Mn, 0.011% P, 0.007% S, 0.019% Al, 0.019% Ti, 0.079% V, 0.0076% N	$A_{c1} = 774\text{ }^{\circ}\text{C}$ $A_{c3} = 877\text{ }^{\circ}\text{C}$	[23]
6.	0.08% C, 0.34% Si, 1.43% Mn, 0.008% P, 0.005% S, 0.014% Al, 0.018% Ti, 0.077% V, 0.0100% N	$A_{c1} = 806\text{ }^{\circ}\text{C}$ $A_{c3} = 871\text{ }^{\circ}\text{C}$	[23]
7.	0.09% C, 0.30% Si, 1.49% Mn, 0.012% P, 0.004% S, 0.02% Al, 0.016% Ti, 0.081% V, 0.0140% N	$A_{c1} = 783\text{ }^{\circ}\text{C}$ $A_{c3} = 868\text{ }^{\circ}\text{C}$	[23]
8.	0.08% C, 0.30% Si, 1.40% Mn, 0.009% P, 0.006% S, 0.023% Al, 0.016% Ti, 0.120% V, 0.0082% N	$A_{c1} = 771\text{ }^{\circ}\text{C}$ $A_{c3} = 877\text{ }^{\circ}\text{C}$	[23]
9.	0.165% C, 0.294% Si, 1.32% Mn, 0.012% P, 0.0007% S, 0.027% Cu, 0.768% Cr, 0.317% Ni, 0.399% Mo, 0.0017% B, 0.003% V, 0.030% Nb, 0.003% Ti	$A_{c1} = 686\text{ }^{\circ}\text{C}$ $A_{c3} = 862\text{ }^{\circ}\text{C}$	[24]
10.	0.072% C, 1.05% Mn, 3.48% Ni, 0.51% Cr, 0.51% Mo, 0.082% V	$A_{c1} = 702\text{ }^{\circ}\text{C}$ $A_{c3} = 820\text{ }^{\circ}\text{C}$	[25]
11.	0.14% C, 0.96% Mn, 0.26% Cr, 1.14% Ni, 0.44% Si, 0.32% Mo i 0.02% Nb	$A_{c1} = 716\text{ }^{\circ}\text{C}$ $A_{c3} = 813\text{ }^{\circ}\text{C}$	[26]
12.	0.15% C, 0.23% Si, 1.30% Mn, 0.017% P, 0.013% S, 0.050% Nb, 0.01% V, 0.012% Ti, 0.09% Cr, 0.019% Ni, 0.025% Al, 0.005% N	$A_{c1} = 714\text{ }^{\circ}\text{C}$ $A_{c3} = 885\text{ }^{\circ}\text{C}$	[27]
13.	0.09% C, 0.18% Si, 1.06% Mn, 0.01% P, 0.003% S, 0.036% Al, 0.002% Nb, 0.007% V, 0.03% Ti, 1.08% Cr, 0.07% Ni, 0.11% Mo.	$A_{c1} = 769\text{ }^{\circ}\text{C}$ $A_{c3} = 855\text{ }^{\circ}\text{C}$	[28]
14.	0.09% C, 0.18% Si, 1.06% Mn, 0.01% P, 0.003% S, 0.036% Al, 0.002% Nb, 0.007% V, 0.03% Ti, 1.08% Cr, 0.07% Ni, 0.11% Mo	$A_{c1} = 773\text{ }^{\circ}\text{C}$ $A_{c3} = 870\text{ }^{\circ}\text{C}$	[29]

state, the microstructure of which consisted mainly of acicular ferrite and cementite, was characterized by higher hardness (234 HV2), yield strength (336 MPa) and tensile strength (589 MPa) than steel after annealing (hardness: 120 HV2, yield strength: 222 MPa, tensile strength: 424 MPa). The authors concluded that the reason for the reduction in hardness after annealing was the homogenization of the microstructure.

CONCLUSIONS

On the basis of the research conducted, the following conclusions can be drawn:

- the A_{c1} temperature for steel in the cast state is 850 °C and the A_{c3} temperature is 950 °C. The

austenitic transformation of this steel begins at a relatively high temperature and is characterized by a quick and violent course;

- in the case of steel in the as-cast state, an increase in the sample length was recorded at a temperature of approximately 730 °C, which was probably caused by the dissolution of the cementite;
- the application of deformation significantly accelerated the onset of the austenitic transformation from a temperature of 850 °C to 750 °C due to the increase in the density of defects, which increased the nucleation rate of the austenitic phase. The A_{c3} temperature for steel after deformation is 940 °C. After applying deformation, the course of the austenitic transformation and the critical temperature values are characteristic for HSLA-type steel;

- as the annealing temperature increases, the hardness increases from 210 HV100 for a temperature of 700 °C to 260 HV100 for a temperature of 920 °C. The exception was a slight decrease in hardness at a temperature of 730 °C, where the hardness was 208 HV100. The slight reduction in hardness may be due to the dissolution of the cementite.

Acknowledgements

Publication supported by the rector's pro-quality grant. Silesian University of Technology, grant number: 32/014/RGJ23/2015.

REFERENCES

1. Zhang Y., Li X., Liu Y., Liu C., Dong J., Yu L., Li H. Study of the kinetics of austenite grain growth by dynamic Ti-rich and Nb-rich carbonitride dissolution in HSLA steel: In-situ observation and modelling. *Materials Characterization* 2020; 169(5): 110612. doi: 10.1016/j.matchar.2020.110612.
2. Shao Y., Liu C., Yan Z., Li H., Liu Y. Formation mechanism and control methods of acicular ferrite in HSLA steels: a review. *Journal of Materials Science & Technology* 2018; 34(5): 737–744. doi: 10.1016/j.jmst.2017.11.020.
3. Opiela M., Grajcar A. Microstructure and anisotropy of plastic properties of thermomechanically-processed HSLA-type steel plates. *Metals* 2018; 8(5): 304. doi: 10.3390/met8050304.
4. Dong J., Li C., Liu C., Huang Y., Yu L., Li H., Liu Y. Microstructural and mechanical properties development during quenching-partitioning-tempering process of Nb-V-Ti microalloyed ultra-high strength steel. *Materials Science and Engineering: A* 2017; 705: 249–256. doi: 10.1016/j.msea.2017.08.081.
5. Jun H., Kang J., Seo D., Kang K., Park C. Effects of deformation and boron on microstructure and continuous cooling transformation in low carbon HSLA steels. *Materials Science and Engineering: A* 2006; 422(1): 157–162. doi: 10.1016/j.msea.2005.05.008.
6. Zavdoveev A., Poznyakov V., Baudin T., Rogante M., Kim H.S., Heaton M., Demchenko Y., Zhukov V., Skoryk M. Effect of heat treatment on the mechanical properties and microstructure of HSLA steels processed by various technologies. *Materials Today Communications* 2021; 28: 102598. doi: 10.1016/j.mtcomm.2021.102598.
7. Málek M., Mičian M., Moravec J. Determination of Phase Transformation Temperatures by Dilatometric Test of S960MC Steel. *Archives of Foundry Engineering* 2021; 21(2): 57-64. doi: 10.24425/afe.2021.136098.
8. Mičian M., Winczek J., Harmaniak D., Koňár R., Gucwa M., Moravec J. Physical simulation of individual heat-affected zones in S960MC steel. *Archives of Metallurgy and Materials* 2021; 66(1): 81–89. doi: 10.24425/amm.2021.134762.
9. Ye Z., Chen G., Wang W., Wang S., Yang J., Huang J. High-strength and high-toughness weld of S690QL HSLA steel via a high-speed high frequency electric cooperated arc welding without additional heating measures. *Materials Science and Engineering: A* 2023; 880: 145328. doi: 10.1016/j.msea.2023.145328.
10. Winarto W., Anis M., Taufiqullah T. Cooling rate control on cold cracking in welded thick HSLA steel plate. *Materials Science Forum* 2011; 689: 269–275. doi: 10.4028/www.scientific.net/MSF.689.269.
11. Wojtacha A., Opiela M. Numerical simulation of the phase transformations in steels: a case study on newly-developed multi-phase steels for drop forgings. *Advances in Science and Technology Research Journal* 2021; 15(1): 126–133. doi: 10.12913/22998624/130863.
12. Morawiec M., Grajcar A., Zalecki W., Garcia-Mateo C., Opiela M. Dilatometric study of phase transformations in 5 Mn steel subjected to different heat treatments. *Materials* 2020; 13(4): 958. doi: 10.3390/ma13040958.
13. Morawiec M., Wojtacha A., Opiela M. Kinetics of austenite phase transformations in newly-developed 0.17C-2Mn-1Si-0.2Mo forging steel with Ti and V microadditions. *Materials* 2021; 14(7): 1698. doi: 10.3390/ma14071698.
14. Kawulok P., Podolinský P., Kajzar P., Schindler I., Kawulok R., Ševčák V., Opéla P. The influence of deformation and austenitization temperature on the kinetics of phase transformations during cooling of high-carbon steel. *Archives of Metallurgy and Materials* 2018; 63(4): 1743–1748. doi: 10.24425/amm.2018.125100.
15. Jandová D., Meyer L., Mašek B., Nový Z., Kešner D., Motyčka P. The influence of thermo-mechanical processing on the microstructure of steel 20MoCrS4. *Materials Science and Engineering: A* 2003; 349(1–2): 36–47. doi: 10.1016/S0921-5093(02)00373-8.
16. Yin S., Sun X., Liu Q., Zhang Z. Influence of Deformation on Transformation of Low-Carbon and High Nb-Containing Steel During Continuous Cooling. *Journal of Iron and Steel Research International* 2010; 17(2): 43–47. doi:10.1016/S1006-706X(10)60057-X.
17. Wang X., Wang Z., Wang X., Wang Y., Gao

- J., Zhao X, Effect of cooling rate and deformation on microstructures and critical phase-transformation temperature of boron-nickel added HSLA h-beams. *Journal of Iron and Steel Research International* 2021; 19(2): 62-66. doi: 10.1016/S1006-706X(12)60061-2.
18. ASTM A1033-04, In Standard Practice for Quantitative Measurement and Reporting of Hypoeutectoid Carbon and Low-Alloy Steel Phase Transformations; ASTM International: West Conshohocken, PA, USA.
19. Dong J., Liu C., Liu Y., Li C., Guo Q., Li H. Effects of two different types of MX carbonitrides on austenite growth behavior of Nb-V-Ti microalloyed ultra-high strength steel. *Fusion Engineering and Design* 2017; 125: 415–422. doi: 10.1016/J.FUSENGDES.2017.05.084.
20. Li X., Liu Y., Gan K., Dong J., Liu C. Acquiring a low yield ratio well synchronized with enhanced strength of HSLA pipeline steels through adjusting multiple-phase microstructures. *Materials Science and Engineering: A* 2020; 785: 139350. doi: 10.1016/j.msea.2020.139350.
21. Ramachandran D., Moon J., Lee C., Kim S., Chung J., Biro E., Park Y. Role of bainitic microstructures with M-A constituent on the toughness of an HSLA steel for seismic resistant structural applications. *Materials Science and Engineering: A* 2021; 801: 140390. doi: 10.1016/j.msea.2020.140390.
22. Hou W., Liu Q., Gu J. Improved impact toughness by multi-step heat treatment in a 1400 MPa low carbon precipitation-strengthened steel. *Materials Science and Engineering: A* 2020; 797(1): 140077. doi: 10.1016/j.msea.2020.140077.
23. Chun X., Sun Q., Chen X. Research on transformation mechanism and microstructure evolution rule of vanadium–nitrogen microalloyed steels. *Materials & Design* 2007; 28(9): 2523–2527. doi: 10.1016/j.matdes.2006.09.005.
24. Chen X., Huang Y. Hot deformation behavior of HSLA steel Q690 and phase transformation during compression. *Journal of Alloys and Compounds* 2015; 619: 564-571. doi: 10.1016/j.jallcom.2014.09.074.
25. Lu J., Yu H., Yang S. Mechanical behavior of multi-stage heat-treated HSLA steel based on examinations of microstructural evolution. *Materials Science and Engineering: A* 2021; 803: 140493. doi: 10.1016/j.msea.2020.140493.
26. Li X., Shi L., Liu Y., Gan K., Liu C. Achieving a desirable combination of mechanical properties in HSLA steel through step quenching. *Materials Science and Engineering: A* 2020; 772(4): 138683. doi: 10.1016/j.msea.2019.138683.
27. Zavdoveev A., Poznyakov V., Baudin T., Rogante M., Kim H.S., Heaton M., Demchenko Y., Zhukov V., Skoryk M. Effect of heat treatment on the mechanical properties and microstructure of HSLA steels processed by various technologies, *Materials Today Communications* 2021; 28: 102598. doi:10.1016/j.mtcomm.2021.102598.
28. Málek M., Mičian M., Moravec J. Determination of phase transformation temperatures by dilatometric test of S960MC steel. *Archives of Foundry Engineering* 2021; 21: 57-64. doi:10.24425/afe.2021.136098.
29. Mičian M., Winczek J., Harmaniak D., Koňár R., Gucwa M., Moravec J. Physical simulation of individual heat-affected zones in S960MC steel. *Archives of Metallurgy and Materials* 2021; 66: 81-89. doi:10.24425/amm.2021.134762.
30. Du L., Liu X., Wang G. The quenching problem in the study of strain induced transformation of low carbon steel. *Acta Metallurgica Sinica* 2002; 38(2): 196–202.
31. Zhou X., Chen Y., Jiang Y., Li Y. Effects of plastic deformation on austenite transformation in Fe-1.93Mn-0.07Ni-1.96Cr-0.35Mo ultra-high strength steel during continuous cooling. *Materials Research Express* 2023; 6: 1–10. doi: 10.1088/2053-1591/ab6e7c.
32. Navarro-Lopez A., Sietsma J., Santofimia M.J.: Effect of prior a thermal martensite on the isothermal transformation kinetic below Ms in a low-C high-Si steel. *Metallurgical and Materials Transactions A* 2016; 47(3): 1028–1039. doi: 10.1007/s11661-015-3285-6.
33. Oliveira B., Oliveira M., Terrones L., M. Gardinieri, Godefroid L. Microstructure and mechanical properties of as-cast and annealed high strength low alloy steel. *Journal of Materials Science Research* 2019; 8(4): 1–13. doi: 10.5539/jmsr.v8n4p1.